

# Bulk chemical characteristics of soluble polar organic molecules formed through condensation of formaldehyde: Comparison with soluble organic molecules in Murchison meteorite

YUKI ISONO,<sup>1</sup> SHOGO TACHIBANA,<sup>1,2\*</sup> HIROSHI NARAOKA,<sup>3</sup> FRANÇOIS-RÉGIS ORTHOUS-DAUNAY,<sup>4</sup> LAURETTE PIANI<sup>5</sup> and YOKO KEBUKAWA<sup>6</sup>

<sup>1</sup>Department of Natural History Sciences, Hokkaido University, N10W8, Sapporo, Hokkaido 060-0810, Japan

<sup>2</sup>UTokyo Organization for Planetary and Space Science, The University of Tokyo, 7-3-1 Hongo, Tokyo 113-0033, Japan

<sup>3</sup>Department of Earth and Planetary Sciences, Kyushu University, 744 Motoooka, Nishi-ku, Fukuoka 819-0395, Japan

<sup>4</sup>Département Mesures Physiques, 17 Quai Claude Bernard, 38000 Grenoble, France

<sup>5</sup>Centre de Recherches Pétrographiques et Géochimiques, 15 rue Notre Dame des Pauvres, 54500 Vandoeuvre-lès-Nancy, France

<sup>6</sup>Faculty of Engineering, Yokohama National University, 79-5 Tokiwadai, Hodogaya-ku, Yokohama 240-8501, Japan

(Received May 24, 2018; Accepted November 20, 2018)

Carbonaceous chondrites contain up to 2 wt% organic carbon, which is present as acid and solvent insoluble solid organic matter (IOM) and solvent soluble organic matter (SOM). The extraterrestrial organic matter should record chemical processes occurred in different environments in the early history of the Solar System, and the role of parent body aqueous alteration in the synthesis or subsequent modification of IOM and SOM still requires accurate constraints. We conducted hydrothermal experiments to simulate the synthesis of organic molecules during aqueous alteration on small bodies. Bulk chemical characteristics of soluble organic matter synthesized from formaldehyde in aqueous solutions were studied to compare them with that of chondritic SOM. We found that the redox state of synthesized organic molecules depends on temperature; the molecules become richer in hydrogen at higher temperatures. This can be explained by a cross-disproportionation reaction between organic molecules and formic acid, which occurs as a side reaction of the aldol condensation and works more effectively at higher temperatures. Comparison of the bulk chemical characteristics between the synthesized molecules and SOM extracted from the Murchison meteorite with methanol shows that the soluble organic molecules in Murchison are more reduced than the synthesized molecules. Considering the temperature condition for aqueous alteration on the CM parent body that is lower than or equivalent to the experimental temperatures, the reduced nature of Murchison organic molecules requires a reducing environment for them to be formed during hydrothermal alteration or imply that processes other than hydrothermal alteration were responsible for their synthesis. In case of hydrothermal synthesis, reducing conditions might be established by the interaction between water and iron-bearing silicates or metals on the parent body.

Keywords: extraterrestrial material, organic matter, meteorite, small body, hydrothermal reaction

## INTRODUCTION

Organic materials in chondrites, micrometeorites and interplanetary dust particles record chemical processes occurred in different environments in the early history of the Solar System such as the Sun's parent molecular cloud, the protosolar disk, and meteorite parent bodies. Carbonaceous chondrites contain up to 2 wt% organic carbon (e.g., Pizzarello *et al.*, 2006). The acid and solvent insoluble organic matter (IOM) accounts for 70–99% of the meteoritic organic carbon, which is considered to be macromolecular and composed of small aromatic moi-

eties combined with short highly branched aliphatic chains and ether linkages (e.g., Derenne and Robert, 2010; Alexander *et al.*, 2017). The residual organic carbon is present as solvent soluble organic matter (SOM). Recent studies of Murchison meteorite with ultrahigh-resolution mass spectroscopy have shown that tens of thousands soluble organic molecules are present in the meteorite (Schmitt-Kopplin *et al.*, 2010; Yamashita and Naraoka, 2014; Naraoka *et al.*, 2017). Various formation pathways have been proposed for the synthesis of extraterrestrial organic matter (Alexander *et al.*, 2017 and references therein); Photo-induced chemistry in molecular clouds (e.g., Piani *et al.*, 2017; Tachibana *et al.*, 2017; Sugahara *et al.*, 2019), Fischer-Tropsch-type synthesis in the solar nebula (e.g., Zolotov and Shock, 2001; Kress and Tielens, 2001), ionization-induced synthesis at high temperature

\*Corresponding author (e-mail: tachi@eps.s.u-tokyo.ac.jp)

(Kuga *et al.*, 2015; Bekaert *et al.*, 2018) and hydrothermal synthesis in meteorite parent bodies (e.g., Cody *et al.*, 2011; Kebukawa *et al.*, 2013, 2017; Kebukawa and Cody, 2015; Koga and Naraoka, 2017).

As the aqueous alteration of the minerals in matrix is unquestionable in Murchison (Rubin *et al.*, 2007) as well as its role in natural organic chemistry (Schulte and Shock, 2004), the typical molecular diversity it can produce has to be investigated in order to find relevant hydrothermal markers in the chondrites organics. Cody *et al.* (2011), Kebukawa *et al.* (2013), and Kebukawa and Cody (2015) experimentally showed that organic solids, synthesized from formaldehyde and ammonia under hydrothermal environments, structurally resemble the chondritic IOM. They concluded that the chondritic IOM could form from simple molecules such as formaldehyde and ammonia, observed in the interstellar medium and comets (e.g., Mumma and Charnley, 2011), due to aqueous activity on chondrite parent bodies. Soluble organic compounds are also synthesized during formaldehyde condensation with ammonia. Kebukawa *et al.* (2017) and Koga and Naraoka (2017) showed that amino acids observed in chondrites could be produced by acid hydrolysis of the aqueous solution after the formaldehyde polymerization reaction with ammonia. However, the whole characteristics of soluble organic matter synthesized from formaldehyde have not yet been fully understood although the bulk chemical information potentially puts constraints on the formation environment and/or scenario. In this study, we focus on bulk chemical characteristics of soluble organic matter synthesized from formaldehyde under hydrothermal conditions to compare them with that of chondritic soluble organic matter.

## METHODS

The hydrothermal organic synthesis experiments were performed following the protocol of Kebukawa *et al.* (2013, 2017) and Kebukawa and Cody (2015). All the glass tubes and spatulas used for the experiments were baked in air at 450°C for 3 hours to combust any environmental organic contaminants. A starting mixture of paraformaldehyde (0.0480 g; Wako Pure Chemical), glycolaldehyde (0.0480 g; Sigma-Aldrich), Ca(OH)<sub>2</sub> (0.0120 g; Wako Pure Chemical), and ultrapure water (800 μL; Milli-Q) were flame sealed in a pyrex glass tube in air with or without ammonia. Ammonia was added as 7.3 wt% ammonia solution (64 μL; Wako Pure Chemical), in order to keep the N/C atomic ratio of the starting material equal to ~0.09. Ca(OH)<sub>2</sub> was added to the system as a catalyst of formaldehyde polymerization and to make the initial solution alkaline (Cody *et al.*, 2011; Kebukawa *et al.*, 2013, 2017; Kebukawa and Cody, 2015). Paraformaldehyde serves as a polymerized source of for-

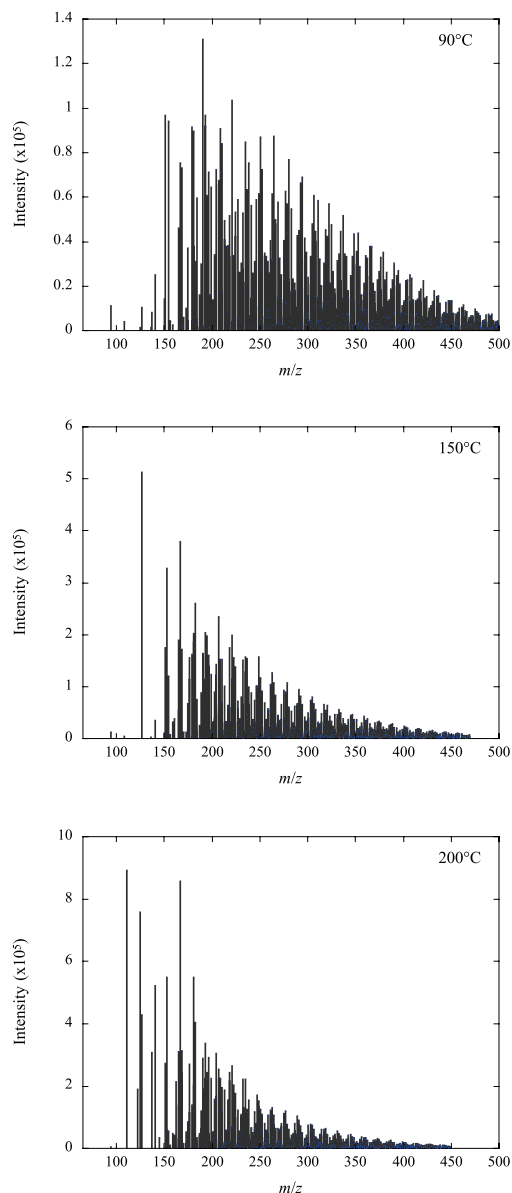


Fig. 1. Typical mass spectra of the assigned molecules from experimental samples (90, 150, and 200°C for 6 days without ammonia).

maldehyde. It is expected to be hydrolyzed and to depolymerize immediately at high pH to yield formaldehyde (Kebukawa *et al.*, 2017). The sealed glass tubes were heated isothermally using electric ovens at 90, 150, and 200°C for 3, 6, and 30 days. The experimental run products were filtrated and diluted 1000 times (by volume) with ultrapure water for liquid-chromatography/high-resolution mass spectrometry.

A high-resolution mass spectrometer (Orbitrap Elite; Thermo Scientific) coupled with nano-liquid-chromato-

Table 1. Number of assigned elemental compositions in the run products

Temperature (°C)	Duration (days)	NH <sub>3</sub>	CHO molecules	CHN molecules	CHNO molecules	Total
90	3	no	461	—	—	461
90	6	no	665	—	—	665
90	30	no	647	—	—	647
90	3	yes	133	16	470	619
90	6	yes	160	17	795	972
90	30	yes	75	31	726	832
150	3	no	668	—	—	668
150	6	no	751	—	—	751
150	3	yes	256	30	790	1076
150	6	yes	277	44	1051	1372
200	3	no	688	—	—	688
200	6	no	776	—	—	776
200	3	yes	252	110	855	1217
200	6	yes	266	116	1012	1394

graph (EASY nLC 1000), installed at Global Research Center for Food & Medical Innovation, Hokkaido University, was used for the analysis. The nano-liquid-chromatography was performed with a reversed-phase ODS (octadecylsilyl C18) column (75  $\mu\text{m}$  in inner diameter and 120 mm in length; particle diameter 3  $\mu\text{m}$ ) with a pre-column. An eluent mixture of the aqueous solution of 0.1% formic acid (A) and the acetonitrile solution of 0.1% formic acid (B) was used as a mobile phase with a flow rate of 300 nL/min. For the samples heated for 3 days, the mobile phase with the mixing ratio of A/B = 99/1 was flowed for the first 3 minutes. The mixing ratio of A and B was changed with a linear gradient from A/B = 99/1 to 1/99 during the following one minute, and the mobile phase with the mixing ratio of A/B = 1/99 continued to be flowed for 15 minutes. For the samples heated for 6 and 30 days, after the 3-minute flow of the mobile phase of A/B = 99/1, the mixing ratio of A and B was changed with a linear gradient from A/B = 99/1 to 1/99 in ten minutes. The mobile phase with the mixing ratio of A/B = 1/99 was flowed for the following 15 minutes. We did not change the mixing ratio of the solutions gradually to focus on the bulk chemical characteristics of the samples. We integrated the total ion current (TIC) chromatograms to obtain bulk compositions of the samples, and the difference in gradient conditions did not affect further discussion. Two- $\mu\text{L}$  of the prepared solution for each sample was injected in total into the Orbitrap mass spectrometer for the analysis.

After separation with nano-liquid-chromatography, the molecules were ionized in positive-mode electrospray ionization (ESI). The capillary voltages were adjusted between 1.6 and 1.8 kV to optimize the signal, depending on the sample. The ion transfer capillary was heated at 200°C, and no gas desolvation was applied. High-resolution mass spectra were acquired over the mass ( $m/z$ )

range of 50–650. The mass resolution was set to 240,000 at  $m/z$  of 400, and the automated gain controller that limits the number of total ions injected to the mass analyser was set to 100,000 ions. Polysiloxane ( $m/z = 445.12003$ ) and diisooctyl phthalate ( $m/z = 391.28429$ ) were used as internal lock masses for mass calibration. The same analysis was made for ultrapure water in each analytical session to clean the column and to check the cleanness of column. The analysis of ultrapure water was repeated if necessary until any residues from samples were eliminated. The data for ultrapure water was used as the analytical blank.

A cumulative average mass spectrum was obtained from a peak of the TIC chromatogram of each sample, which was used to assign molecular compositions and obtain bulk compositions of the samples. The bulk compositions of SOMs including volatile molecules can be obtained directly with this technique. The cumulative average mass spectrum was analysed with the software ATTRIBUTOR that works on IGOR pro (e.g., Briois *et al.*, 2016).

## RESULTS

### Total ion current chromatogram of synthesized molecules

The TIC chromatograms of the Orbitrap analysis showed that total ion intensities for all experimental samples were larger than those of blank analysis measured in the same analytical session. This clearly suggests that soluble organic molecules formed under all experimental conditions. Larger TICs were obtained for the samples heated at higher temperatures for the same duration, i.e., more efficient synthesis of organic molecules at higher temperatures. We will not discuss the details of molecules polarity and the effect on their retention time because we focus on the bulk characteristics of a group of molecules

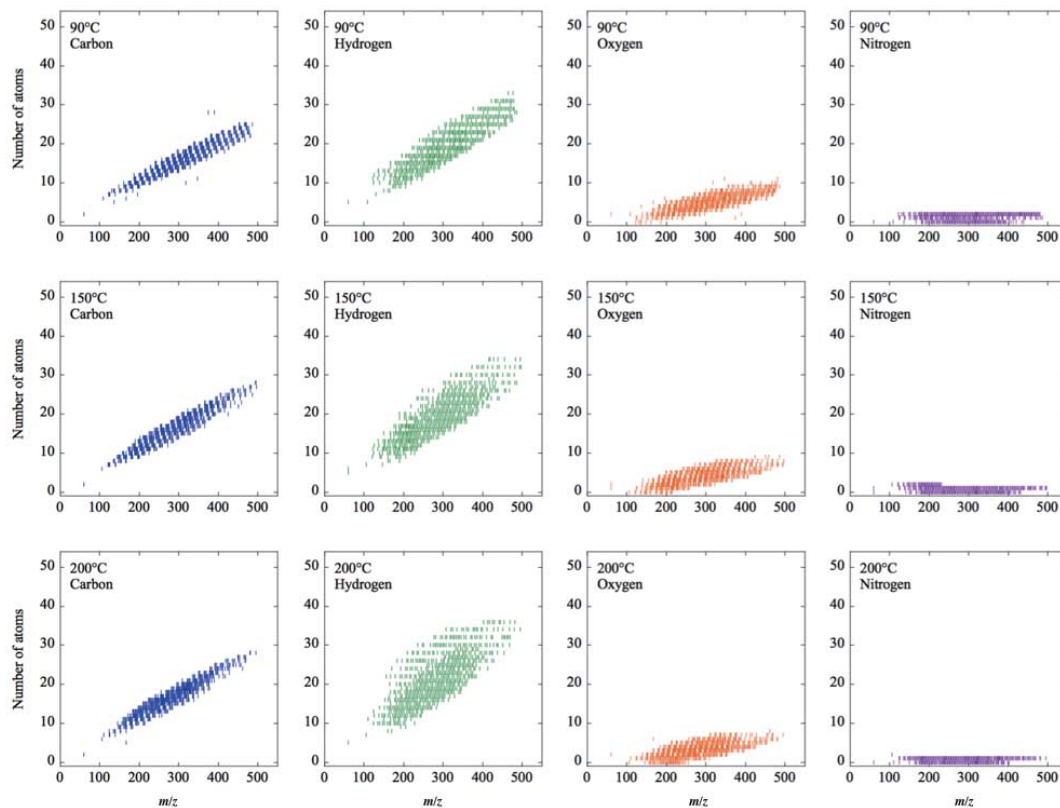


Fig. 2. Numbers of carbon, hydrogen, oxygen, and nitrogen atoms in the molecules synthesized at 90, 150, and 200°C for 6 days with ammonia.

and because the nano-liquid-chromatography used in this study could not well separate individual molecules.

#### Assignment of organic molecules synthesized under hydrothermal conditions

The cumulative average mass spectra of the samples have  $\sim 10^4$  peaks in the  $m/z$  range of 50–650. The peak intensities span a range of 3–4 orders of magnitude, and the 3,000 most intense peaks were first selected to assign molecular compositions and to study the bulk chemical properties of the soluble organic matter synthesized under different conditions. We did not include peaks with  $m/z > 500$  for the assignment of molecular compositions because there are a large number of possible compositional formulas that may enhance the possibility of misassignment (Kujawinski and Behn, 2006). The molecules with  $m/z > 500$  are minor among the synthesized molecules, and this procedure does not affect the estimate of the bulk composition of the whole group of molecules.

Molecular compositions of the 3,000 most intense peaks were assigned as  $C_xH_yO_z$  and  $C_xH_yO_zN_w$  for the experimental products synthesized without and with am-

Table 2. Bulk elemental H/C, O/C, and N/C ratios of the synthesized molecules

Temperature (°C)	Duration (days)	NH <sub>3</sub>	H/C	O/C	N/C
90	3	no	1.10	0.39	—
90	6	no	1.11	0.38	—
90	30	no	1.11	0.36	—
90	3	yes	1.21	0.25	0.12
90	6	yes	1.21	0.27	0.12
90	30	yes	1.22	0.24	0.13
150	3	no	1.15	0.29	—
150	6	no	1.16	0.30	—
150	3	yes	1.17	0.22	0.08
150	6	yes	1.18	0.22	0.09
200	3	no	1.24	0.23	—
200	6	no	1.23	0.24	—
200	3	yes	1.26	0.16	0.08
200	6	yes	1.26	0.17	0.08

monia, respectively. The molecular compositions were determined to satisfy the following requirements, assuming that the  $m/z$  of a peak represents that of a protonated positive ion of a molecule: (1) all electrons are paired,

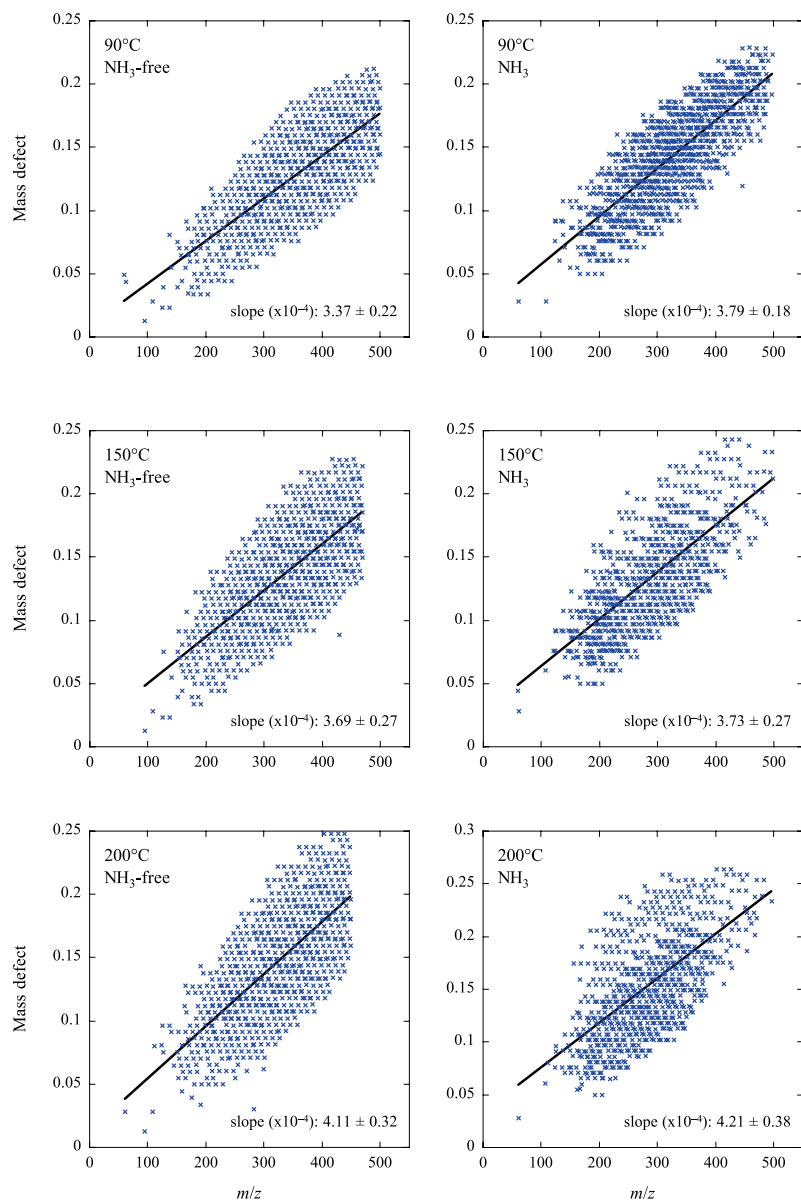


Fig. 3. MDvEM diagrams of the molecules synthesized at 90, 150, and 200 °C for 6 days with ammonia. The linear trends of data are shown as solid lines.

(2) a molecule contains at least one carbon atom ( $x > 1$ ), (3) a molecule contains at least one oxygen or nitrogen because hydrocarbons are not well detected in the present analytical conditions and are not soluble to water, and (4) the mass calibration tolerance is  $\pm 3$  ppm. The estimated compositions were further examined with the following constraints to eliminate molecules with peculiar compositions: (1) O/C and N/C ratios should be  $\leq 3$ , and (2) the number of N in a molecule should be  $\leq 5$ , and (3) the intensity of a peak should be more than 10 times larger than that of the same peak observed in the blank analy-

sis. We set the limitations (1) and (2) empirically because appropriate chemical formulas cannot be found with O/C and N/C  $> 3$  or the number of N  $> 5$ .

For the samples synthesized from the ammonia-bearing solution, there may be more misassigned molecules because of the increase of a compositional parameter (nitrogen). We filtered out possible misassigned molecular compositions by the following procedure; the peaks in a sample heated under the same conditions without ammonia were assigned as  $C_xH_yO_zN_w$  molecules with the same procedure described above. If the same N-bearing mo-

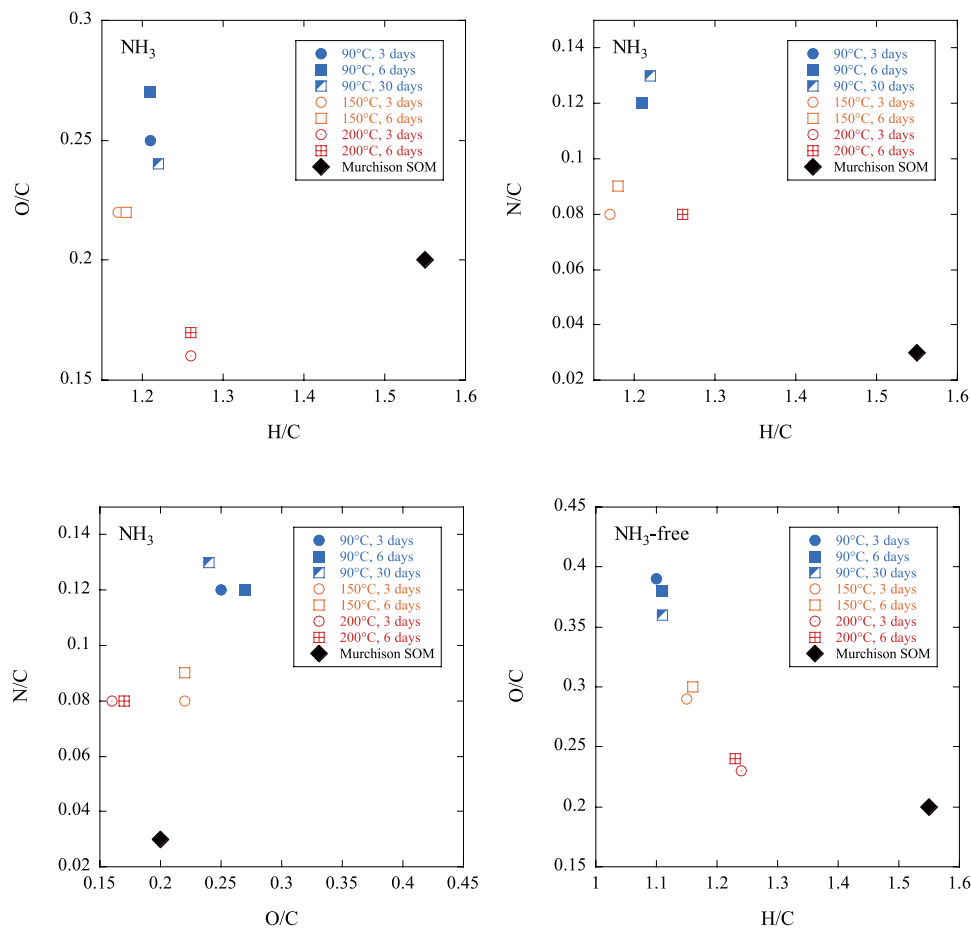


Fig. 4. Bulk H/C, O/C, and N/C ratios of the molecules synthesized at 90, 150, and 200°C with and without ammonia. The elemental ratios of Murchison methanol extract are also shown for comparison (Schmitt-Kopplin et al., 2010).

Table 3. Oxidation states of carbon in the synthesized molecules and the H/C, O/C, and N/C ratios of the growth unit

Temperature (°C)	Duration (days)	NH <sub>3</sub>	Oxidation state of C	(H/C) <sub>growth unit</sub>	(O/C) <sub>growth unit</sub>
90	3	no	-0.32	1.13 ± 0.08*	0.44 ± 0.03*
90	6	no	-0.35	1.21 ± 0.07	0.48 ± 0.03
90	30	no	-0.39	1.22 ± 0.07	0.46 ± 0.03
90	3	yes	-0.35	1.19 ± 0.07	0.41 ± 0.04
90	6	yes	-0.31	1.20 ± 0.06	0.42 ± 0.03
90	30	yes	-0.35	1.22 ± 0.06	0.46 ± 0.03
150	3	no	-0.57	1.16 ± 0.07	0.37 ± 0.03
150	6	no	-0.56	1.22 ± 0.08	0.43 ± 0.03
150	3	yes	-0.25	1.12 ± 0.05	0.35 ± 0.02
150	6	yes	-0.47	1.11 ± 0.06	0.35 ± 0.02
200	3	no	-0.78	1.19 ± 0.07	0.34 ± 0.02
200	6	no	-0.75	1.23 ± 0.08	0.36 ± 0.03
200	3	yes	-0.70	1.15 ± 0.07	0.30 ± 0.02
200	6	yes	-0.68	1.15 ± 0.08	0.29 ± 0.03

\*All errors are 2-sigma.

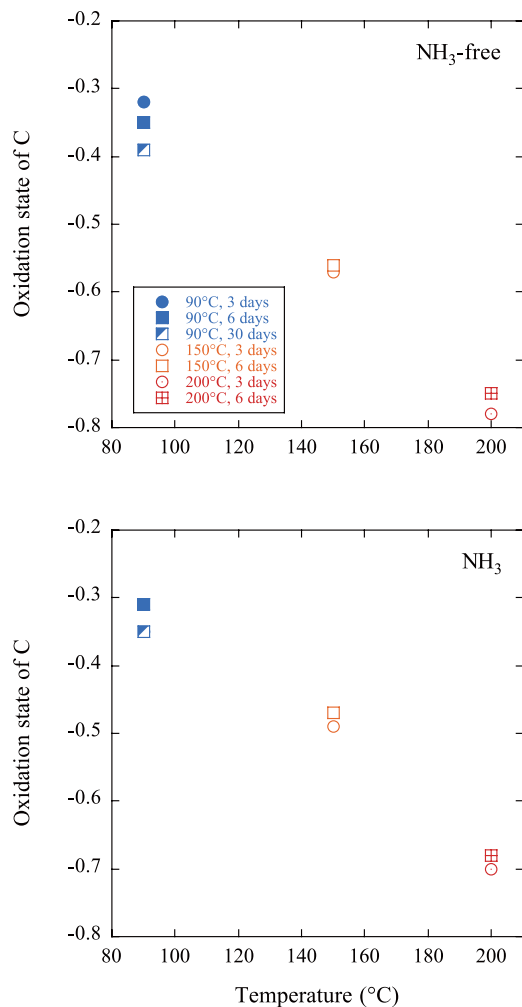


Fig. 5. Temperature dependence of oxidation state of carbon in the molecules synthesized with and without ammonia.

lecular composition was assigned for the samples both with and without ammonia and its peak intensity in the sample with ammonia was not ten times larger than that in the sample without ammonia, it was discarded as a misassigned molecular composition.

In total, molecular compositions of more than several hundreds of peaks were assigned out of 3,000 intense peaks (Fig. 1; Table 1). The numbers of CHO, CHN, and CHON molecules are also listed in Table 1. CHON molecules clearly dominate over CHN molecules in the samples heated with ammonia and that the relative abundance of CHN molecules to CHON molecules increases with temperature.

The numbers of carbon, hydrogen, oxygen, and nitrogen in each molecule in the samples heated at 90, 150, and 200°C for 6 days are plotted against  $m/z$  in Fig. 2. The numbers of carbon, hydrogen, and oxygen increase

with  $m/z$  for the molecules synthesized in this study, while no clear trend was seen for nitrogen.

#### Mass defect vs. exact mass (MDvEM) diagrams

The mass defect for each molecular composition is defined as a decimal number ranging from  $-0.5$  to  $0.5$  that is given as the difference between the exact mass of a molecule and the closest integer. The mass defects of all assigned molecules are plotted against the exact masses in Fig. 3 (MDvEM diagrams; Danger *et al.*, 2013). A trend line observed in the MDvEM diagram represents a specific repetitive pattern in the group of molecules such as  $\text{CH}_2$  and  $\text{C}_2\text{H}_2\text{O}$ , which should be related to the synthetic pathway of the molecules (Danger *et al.*, 2013). We observed trend lines in MDvEM diagrams for all the samples synthesized at different temperatures (Fig. 3). The global slopes for the molecules formed at higher temperatures are steeper than those for the samples at lower temperatures. The molecules formed in the presence of ammonia also tend to have steeper slopes than those formed without ammonia.

#### Bulk elemental ratios of synthesized molecules

The bulk H/C, O/C and N/C ratios of synthesized molecules were obtained by averaging the elemental compositions of assigned molecules using their peak intensities as weights. It has been shown that the intensity-weighted average compositions obtained by ESI positive and negative modes are in close agreement ( $\pm 15\%$ ) with the bulk composition determined by combustion elemental analysis (Hockaday *et al.*, 2009).

The obtained bulk H/C ratios of the synthesized molecules without ammonia are 1.10–1.11, 1.15–1.16, and 1.23–1.24 for the samples heated at 90, 150 and 200°C, respectively, and tend to increase with temperature (Table 2; Fig. 4). The bulk O/C ratios of the synthesized molecules without ammonia tend to decrease with temperature, and are estimated to be 0.36–0.39, 0.29–0.30, and 0.23–0.24 for the molecules formed at 90, 150 and 200°C, respectively. No significant time dependence was found in the bulk H/C and O/C ratios.

Similar temperature dependence was observed for the bulk O/C and H/C ratios of the molecules synthesized with ammonia (Table 2; Fig. 4) except for that the bulk H/C ratio of the molecules formed at 150°C is lower than that at 90°C, which should be focused on future studies. The bulk N/C ratio of the molecules synthesized tends to decrease with temperature (Table 2).

## DISCUSSION

#### Oxidation states of carbon in synthesized molecules and average growth units

The average oxidation states of carbon in the mol-

ecules synthesized at different conditions are calculated from the bulk elemental ratios as  $-[(+1) \times (\text{H}/\text{C}) + (-2) \times (\text{O}/\text{C}) + (-3) \times (\text{N}/\text{C})]$ , where oxidation states of hydrogen, oxygen and nitrogen are given as +1, -2 and -3, respectively (Table 3; Fig. 5) (e.g., Kroll *et al.*, 2011). The oxidation state of -3 was chosen for nitrogen because nitrogen was added in the system as  $\text{NH}_3$  and because little or no presence of N-O bonds in organic solids, synthesized with the same protocol (Kebukawa *et al.*, 2013), suggests that nitro compounds are less abundant than other N-bearing species. The oxidation states of carbon in the molecules formed both with and without ammonia tend to be more negative for the molecules synthesized at higher temperatures. This indicates that more reduced molecules formed at higher temperatures.

The trends of increments of elements in molecules against  $m/z$  (Fig. 2) give an overall growth direction, i.e., an average elemental composition of the growth unit, during molecular synthesis. The average compositions of the growth unit for the synthesized molecules were estimated from the linear regressions of increments of C, H, and O against  $m/z$  (Table 3). It is clearly seen that the growth unit at higher temperatures contains less oxygen than that at lower temperatures.

#### *Bulk chemical characteristics of soluble organic molecules in hydrothermal synthesis*

The bulk chemical characteristics of the synthesized molecules changed with temperature (Figs. 2–5; Tables 1–3); (1) the bulk H/C ratio increases with temperature, (2) the bulk O/C ratio decreases with temperature, (3) the relative abundance of CHN molecules to CHON molecules increases with temperature, (4) the oxidation state of carbon decreases with temperature, (5) the slope in the MDvEM diagram is steeper at higher temperatures, and (6) the average composition of the growth unit is depleted in O at higher temperatures. These lines of evidences strongly suggest that more reduced molecules formed at higher temperatures.

Oligomerization and polymerization of formaldehyde has been known as the formose reaction, where aldose and ketose sugars formed through the aldol condensation of formaldehyde (e.g., Breslow, 1959), resulting in sugar synthesis. The main reaction pathway consists of addition of formaldehyde and subsequent dehydration, and the oxidation state of carbon does not change through these reactions.

A side reaction that changes the oxidation state of carbon is required to explain the synthesis of reduced molecules, which is likely to be the non-catalysed Cannizzaro reaction of formaldehyde (Morooka *et al.*, 2005, 2008). Formic acid (oxidation number of C: +2) and methanol (oxidation number of C: -2) form through a disproportionation reaction of formaldehyde (oxidation

number of C: 0). Formic acid has a strong reducing ability under hydrothermal conditions to react with formaldehyde to form methanol (oxidation number of C: -2) and  $\text{CO}_2$  (oxidation number of C: +4) (cross-disproportionation reaction). Because  $\text{CO}_2$  is removed from the reaction system as gas, the synthesized molecules should be more reduced when the cross-disproportionation reaction works effectively in the reaction system. The cross-disproportionation reaction has larger activation energy than the aldol condensation reaction, and it works more effectively at higher temperatures (Morooka *et al.*, 2008). Kebukawa *et al.* (2013), who synthesized chondritic IOM-like solid organics under the same experimental conditions, also discussed that decrease of pH during their experiments partly to the Cannizzaro reaction.

Kebukawa *et al.* (2013) analysed organic solids synthesized in the same system with solid-state  $^{13}\text{C}$  NMR (Nuclear Magnetic Resonance) spectroscopy, FTIR (Fourier Transform Infrared) micro-spectroscopy, and XANES (X-ray Absorption Near Edge Structure) spectroscopy, and showed that the C=C and  $\text{CH}_x$  functional groups increase in the structure of organic solids with temperature, while the  $\text{CH}_x\text{O}$  (alcohol and/or ether), C=C-O, and C=O functional groups decreased in the organic structure. They also showed that the bulk O/C ratio of the organic solid decreases with temperature. These observations indicate that the organic solid formed under hydrothermal conditions becomes more reduced with increasing temperature, which is consistent with the trend for soluble organic molecules observed in the present study.

No significant time dependence of chemical compositions indicates that the bulk chemical composition of the solution reaches a steady state in 3 days. It is consistent with the observation that the molecular structure of organic solids did not show significant changes with time after 3 days at  $90^\circ\text{C}$  (Kebukawa and Cody, 2015). However, the yields of organic solids increased at least until 11 days at  $90^\circ\text{C}$ , both with and without ammonia (Kebukawa *et al.*, 2013). This indicates that synthesis of water-insoluble organic solid proceeds in a solution with the steady-state chemical composition.

#### *Comparison with the bulk chemical characteristics of Murchison methanol extract*

Schmitt-Kopplin *et al.* (2010) analysed SOMs extracted from Murchison by methanol using electrospray ionization (ESI) Fourier transform ion cyclotron resonance/mass spectrometry (FTICR/MS). The bulk composition of the Murchison methanol extract, analysed in the negative mode, was calculated to be  $\text{C}_{100}\text{H}_{155}\text{O}_{20}\text{N}_3\text{S}_3$  based on the assigned molecular compositions and the peak intensities. As mentioned above, the bulk H/C, O/

C, and N/C ratios for the intensity-weighted average compositions obtained by ESI positive and negative modes are in close agreement with those determined by elemental analysis ( $\pm 15\%$ ; Hockaday *et al.*, 2009).

The bulk H/C, O/C, and N/C ratios of the Murchison methanol extract (Schmitt-Kopplin *et al.*, 2010) are compared with those of the synthesized molecules at 90, 150, and 200°C (Fig. 4). The bulk H/C ratio of the Murchison methanol extract is larger than any of the organic mixtures synthesized in the present study, which the bulk N/C ratio of the Murchison methanol extract is smaller than those in the present study. The bulk O/C ratio of the Murchison methanol extract is close to those of the molecules synthesized at 150 and 200°C with ammonia, while it is smaller than those of the molecules synthesized without ammonia.

The high H/C ratio and low N/C and O/C ratios of the bulk Murchison methanol extract indicate that they are more reduced than the synthesized molecules, and that the molecules synthesized in the present study cannot simply explain the bulk chemical characteristics of the Murchison chondrite SOM. The reduced nature of the Murchison SOMs implies that the synthesis of the Murchison SOMs required either temperature of  $\geq 150$ –200°C or hydrogen-rich reduced solution, or both, if they formed under hydrothermal conditions on the parent body.

The alteration temperature of the CM2 parent body is estimated to be lower than 25–33°C (Zolensky *et al.*, 1989; Guo and Eiler, 2007). Verdier-Paoletti *et al.* (2017) recently estimated the average formation temperatures of carbonates and serpentine in the CM parent bodies to be 110 and 75°C, respectively, and argued that the carbonate formation temperature of Murchison is  $\sim 150$ °C. In either case, the temperature of higher than 150–200°C may not be expected on the Murchison parent body. If this was the case, molecular synthesis under a reduced environment would be responsible for the bulk chemical characteristics of the Murchison SOMs. A possible way to form a reducing environment would be aqueous alteration of silicate minerals and/or oxidation of metals. For instance, serpentinization of iron-bearing olivine results in generation of hydrogen gas, which could be a reducing agent for hydrothermal organic synthesis on the Murchison parent body. This hypothesis should be experimentally investigated under asteroidal hydrothermal conditions in future studies.

Alternatively, the present study may imply that Murchison SOMs were not synthesized by the hydrothermal activity that was shown to be a possible pathway to form IOM-like organic compounds on a parent body (Kebukawa *et al.*, 2013). If this is the case, processes other than hydrothermal alteration on the parent body (possibly prior to planetesimal formation) might have been responsible for the synthesis of Murchison SOMs (e.g., photochemistry in molecular clouds).

## CONCLUSIONS

Bulk chemical characteristics of soluble organic molecules synthesized from formaldehyde under hydrothermal conditions were investigated to understand the reaction pathway and to compare them with that of chondritic soluble organic matter. No significant time dependence was found in the bulk chemistry of the synthesized molecules for samples heated at 90°C for 3–30 days and at 150 and 200°C for 3–6 days. Clear temperature dependence of the bulk chemical characteristics was found; (1) the bulk H/C ratio increases with temperature, (2) the bulk O/C ratio decreases with temperature, (3) the relative abundance of CHN molecules to CHON molecules increases with temperature, (4) the oxidation state of carbon decreases with temperature, (5) the slope in the MDvEM diagram is steeper at higher temperatures, and (6) the average composition of the growth unit is depleted in O at higher temperatures. All of these characteristics suggest the effective formation of more reduced molecules at higher temperatures. Polymerization of formaldehyde through the aldol condensation does not change the oxidation state of carbon in the molecules, and it cannot solely explain the synthesis of reduced molecules. The cross-disproportionation reaction by formic acid that takes a part of carbon out from the reaction system as CO<sub>2</sub> is a process responsible for the synthesis of reduced molecules. The cross-disproportionation reaction works effectively at higher temperatures, which can also explain the production of more reduced molecules at higher temperatures.

The bulk chemical characteristics of soluble organic molecules extracted by methanol from Murchison CM2.5 chondrite are more reduced than those of the molecules synthesized in this study. The reduced nature of the Murchison methanol extract could be explained by the hydrothermal reaction in the present experimental system at  $\geq 150$ –200°C, but the aqueous alteration on the Murchison parent body may not have occurred at such high temperatures. If hydrothermal process on the Murchison parent body was solely responsible for the molecular synthesis and other processes did not contribute the SOM synthesis, the reduced soluble organic molecules in Murchison could have been synthesized in a more reducing environment, which could be established by aqueous alteration of silicate minerals and/or oxidation of metals.

**Acknowledgments**—We thank Iyo Sugawara for her help in analysis of synthesized samples. Itsuro Sugimura is thanked for his technical assistance and helpful suggestions. Constructive reviews by Hikaru Yabuta and an anonymous reviewer are greatly appreciated.

## REFERENCES

- Alexander, C. M. O'D., Cody, G. D., De Gregorio, B. T., Nittler, L. R. and Stroud R. M. (2017) The nature, origin and modification of insoluble organic matter in chondrites, the major source of Earth's C and N. *Chem. der Erde* **77**, 227–256.
- Bekaert, D. V., Derenne, S., Tissandier, L., Marrocchi, Y., Charnoz, S., Anquetil, C. and Marty, B. (2018) High-temperature ionization-induced synthesis of biologically relevant molecules in the protosolar nebula. *Astrophys. J.* **859**, 142 (12 pp.).
- Breslow, R. (1959) On the mechanism of the formose reaction. *Tetrahedron Lett.* **21**, 22–26.
- Briois, C., Thissen R., Thirkell, L., Aradj, K., Bouabdellah, A., Boukrara, A., Carrasco, N., Chalumeau, G., Chapelon, O., Colin, F., Coll, P., Cottin, H., Engrand, C., Grand N., Lebreton, J.-P., Orthous-Daunay, F.-R., Pennanech, C., Szopa, C., Vuitton, V., Zapf, P. and Makarov, A. (2016) Orbitrap mass analyzer for in situ characterization of planetary environments: Performance evaluation of a laboratory prototype. *Planet. Space Sci.* **131**, 33–45.
- Cody, G. D., Heying, E., Alexander, C. M. O'D., Nittler, L. R., Kilcoyne, A. L. D., Standford, S. A. and Stroud, R. M. (2011) Establishing a molecular relationship between chondritic and cometary organic solids. *Proc. Natl. Acad. Sci.* **108**, 19171–19176.
- Danger, G., Orthous-Daunay, F.-R., de Marcellus, P., Modica, P., Vuitton, V., Duvernay, F., Flandinet, L., Le Sergeant d'Hendecourt, L., Thissen, R. and Chivassa, T. (2013) Characterization of laboratory analogs of interstellar/cometary organic residues using very high resolution mass spectrometry. *Geochim. Cosmochim. Acta* **118**, 184–201.
- Derrene, S. and Robert, F. (2010) Model of molecular structure of the insoluble organic matter isolated from Murchison meteorite. *Meteorit. Planet. Sci.* **45**, 1461–1475.
- Guo, W. and Eiler, J. M. (2007) Temperatures of aqueous alteration and evidence for methane generation on the parent bodies of the CM chondrites. *Geochim. Cosmochim. Acta* **71**, 5565–5575.
- Hockaday, W. C., Purcell, J. M., Marshall, A. G., Baldock, J. A. and Hatcher, P. G. (2009) Electrospray and photoionization mass spectrometry for the characterization of organic matter in natural waters: a qualitative assessment. *Limnol. Oceanogr.* **7**, 81–95.
- Kebukawa, Y. and Cody, G. D. (2015) A kinetic study of the formation of organic solids from formaldehyde: Implications for the origin of extraterrestrial organic solids in primitive Solar System objects. *Icarus* **248**, 412–423.
- Kebukawa, Y., Kilcoyne, A. L. D. and Cody, G. D. (2013) Exploring the potential formation of organic solids in chondrites and comets through polymerization of interstellar formaldehyde. *Astrophys. J.* **771**, 19–30.
- Kebukawa, Y., Queenie, H. S. C., Tachibana, S., Kobayashi, K. and Zolensky, M. E. (2017) One-pot synthesis of amino acid precursors with insoluble organic matter in planetesimals with aqueous activity. *Sci. Adv.* **3**, e1602093.
- Koga, T. and Naraoka, H. (2017) A new family of extraterrestrial amino acids in the Murchison meteorite. *Sci. Rep.* **7**, doi:10.1038/s41598-017-00693-9.
- Kress, M. E. and Tielens, A. G. G. M. (2001) The role of Fischer-Tropsch catalysis in solar nebula chemistry. *Meteor. Planet. Sci.* **36**, 75–92.
- Kroll, J. H., Donahue, N. M., Jimenez, J. L., Kessler, S. H., Canagaratna, M. R., Kevin, R., Wilson, K. R., Altieri, K. E., Mazzoleni, L. R., Wozniak, A. S., Bluhm, H., Mysak, E. R., Smith, J. D., Kolb, C. E. and Worsnop, D. R. (2011) Carbon oxidation state as a metric for describing the chemistry of atmospheric organic aerosol. *Nat. Chem.* **3**, 133–139.
- Kuga, M., Marty, B., Marrocchi, Y. and Tissandier, L. (2015) Synthesis of refractory organic matter in the ionized gas phase of the solar nebula. *Proc. Natl. Acad. Sci. USA* **112**, 7129–7134.
- Kujawinski, E. B. and Behn, M. D. (2006) Automated analysis of electrospray ionization fourier transform ion cyclotron resonance mass spectra of natural organic matter. *Anal. Chem.* **78**, 4363–4373.
- Morooka, S., Wakai, C., Matsubayashi, N. and Nakahara, M. (2005) Hydrothermal Carbon-Carbon formation and disproportionation reaction of C1 aldehyde: Fromaldehyde and formic acid. *J. Phys. Chem. A* **109**, 6610–6619.
- Morooka, S., Matsubayashi, N. and Nakahara, N. (2008) Hydrothermal C-C bond formation and disproportionation of aldehyde with formic acids. *J. Phys. Chem. A* **112**, 6950–6959.
- Mumma, M. J. and Charnley, S. B. (2011) The chemical composition of comets—Emerging taxonomies and natal heritage. *Ann. Rev. Astron. Astrophys.* **49**, 471–524.
- Naraoka, H., Yamashita, Y., Yamaguchi, M. and Orthous-Daunay, F.-R. (2017) Molecular evolution of N-containing cyclic compounds in the parent body of the Murchison meteorite. *ACS Earth Space Chem.* **9**, 540–550.
- Piani, L., Tachibana, S., Hama, T., Tanaka, H., Endo, Y., Sugawara, I., Dessimoulie, L., Kimura, Y., Miyake, A., Matsuno, J., Tsuchiyama, A., Fujita, K., Nakatsubo, S., Fukushi, H., Mori, S., Chigai, T., Yurimoto, H. and Kouchi, A. (2017) Evolution of morphological and physical properties of laboratory interstellar organic residues with ultraviolet irradiation. *Astrophys. J.* **837**, 35 (11 pp.).
- Pizzarello, S., Cooper, G. W. and Flynn, G. J. (2006) The nature and distribution of the organic material in carbonaceous chondrites and interplanetary dust particles. *Meteorites and the Early Solar System II* (Lauretta, D. S. and McSween, H. Y., eds.), 625–651, Univ. Arizona Press.
- Rubin, A. E., Trigo-Rodríguez, J. M., Huber, H. and Wasson, J. T. (2007) Progressive aqueous alteration of CM carbonaceous chondrites. *Geochim. Cosmochim. Acta.* **71**, 2361–2382.
- Schmitt-Kopplin, P., Gabelica, Z., Gougeon, R. D., Fekete, A., Kanawati, B., Harir, M., Gebefuegi, I., Eckel, G. and Hertkorn, N. (2010) High molecular diversity of extraterrestrial organic matter in Murchison meteorite revealed 40 years after its fall. *Proc. Natl. Acad. Sci.* **107**, 2763–2768.
- Schulte, M. and Shock, E. (2004) Coupled organic synthesis and mineral alteration on meteorite parent bodies. *Meteorit. Planet. Sci.* **39**, 1577–1590.

- Sugahara, H., Takano, Y., Tachibana, S., Sugawara, I., Chikaraishi, Y., Ogawa, N. O., Ohkouchi, N., Kouchi, A. and Yurimoto, H. (2019) Molecular and isotopic compositions of nitrogen-containing organic molecules formed during UV-irradiation of simulated interstellar ice. *Geochem. J.* **53**, this issue, 5–20.
- Tachibana, S., Kouchi, A., Hama, T., Oba, Y., Piani, L., Iyo S., Endo, Y., Hidaka, H., Kimura, Y., Murata, K., Yurimoto, H. and Watanabe, N. (2017) Liquid-like behavior of UV-irradiated interstellar ice analog at low temperatures. *Sci. Adv.* **3**, eaao2538.
- Verdier-Paoletti, M. J., Marrocchi, Y., Avice, G., Roskosz, M., Gurenko, A. and Gounelle, M. (2017) Oxygen isotope constraints on the alteration temperatures of CM chondrites. *Earth Sci. Planet. Lett.* **458**, 273–281.
- Yamashita, Y. and Naraoka, H. (2014) Two homologous series of alkylpyridines in the Murchison meteorite. *Geochem. J.* **48**, 519–525.
- Zolensky, M. E., Bourcier, W. L. and Gooding, J. L. (1989) Aqueous alteration on the hydrous asteroids: Results of EQ3/6 computer simulations. *Icarus* **78**, 411–425.
- Zolotov, M. Y. and Shock, E. L. (2001) Stability of condensed hydrocarbons in the solar nebula. *Icarus* **150**, 323–337.